Structure modeling and dynamics driven mutation and phosphorylation analysis of Beta-amyloid peptides

Sunil Kumar Singh, Ankita Singh, Ved Prakash* & C. Selvaa Kumar

Department of Biotechnology and Bioinformatics, padmashree Dr.D.Y.Patil University, Belapur-400614, Navi Mumbai, India; Ved Prakash - Email: Ved.prakash2012@vit.ac.in; Phone: +917845793794; *Corresponding author

Abstract:
The most common characteristics of diverse age-related neurodegenerative diseases are aggregation and accumulation of the misfolded protein in the brain. Alzheimer's disease (AD) is one of these protein conformational diseases. Extracellular accumulation of amyloid β (Aβ) is one the neuropathological hallmarks of Alzheimer disease. Various studies have shown that mutation in specific hydrophobic region of Aβ protein inhibit the formation of β sheet, thus aggregation of this protein is stalled. The identification of such mutation in Aβ protein can help us in elucidating the etiology of sporadic Aβ. In our study we have selected three positions: 19ILU, 21ALA and 41ILU in Aβ protein based on their hydrophobic nature and substituted them with PRO (βSheet breaker). The effects of the substitutions were analysed using molecular dynamics simulation studies. The results validated that the mutations in the specified regions change the hydrophobicity of the protein and the βsheet formation was declined to zero per cent.

Keywords: Alzheimer's disease, Amyloid-beta precursor protein, Amyloid-beta peptide, Gromos, PPI-Pred, Argus Lab, UCSF Chimera.

Background:
Age-related impairments in cognition and memory have been known since ancient times, but the clinical pathological features of the syndrome, now termed "Alzheimer's disease" (AD), were not documented in the medical literature until the first decade of this century. It is now established that AD is a complex and genetically heterogeneous, neurodegenerative disorder. It is the most common type of dementia. Dementia is derived from the Latin word, [de-=out from + mentia=the mind] means loss or impairment of mental powers due to a disease. There is no cure for AD till today, however promising research and development for early detection and treatment is underway.

Plaques and Tangles: The Hallmarks of AD
The brains of people with AD have an abundance of two abnormal structures:

- Amyloid Beta (Aβ) plaques build up between nerve cells. They contain deposits of (Aβ), a protein fragment.
- Neurofibrillary tangles, which are twisted fibers that build up inside the nerve cell.

Amyloid Precursor Protein (APP) can be processed by at least three secretases: α-, β-, and ϒ-secretases [1, 2]. Cleavage of APP by an 'α-secretase' enzyme (a member of the ADAM family of metalloproteases) [3] occurs within the, Aβ sequence, and results in the secretion of an approx. 100 kDa N-terminal fragment [1]. On the other hand, intact, Aβ is derived from APP by cellular processing pathways that involve the excision of the, Aβ region by the sequential action of 'β,-' and 'γ-secretase' enzymes, possibly in distinct subcellular compartments [4]. β-secretase (a membranebound aspartyl protease also called BACE) cleave the ectodomain of APP, resulting in the shedding

of APPsα and APPsβ (12 kDA). The 12-kd fragment may then undergo γ -secretase cleavage within the hydrophobic transmembrane domain at either valine 710, alanine 712, or threonine 713 to release the 40, 42, or 43 residue Aβ peptides. The strongest evidence that abnormal proteolytic processing and increased Aβ generation are central to the disease process comes from studies of very rare inherited forms of AD **[3].**

Amyloid-β Peptide Conformations: Monomers
The Aβ is a peptide that is ubiquitously and normally expressed in humans predominately in two forms, 39- and 43- amino acids in length (Aβ40 and Aβ42, respectively) **[5, 6,].** Monomers are about 1.0 ± 0.3 nm in size, with a molecular weight of: 4329.9 Da for Aβ (1-40) and 4514.1 Da for Aβ (1-42). Monomers present mostly random coils and α-helix secondary structures. Two α-helical regions exist at residues 8-25 and 28-38, and these regions are separated by a flexible hinge. The rest of the peptide adopts random coil-like conformation **[7].**

Common Pathways of Aggregation amyloid-β peptide
The earliest event in the process of aggregation is the formation of dimmers. Aβ derived from a segment of APP is believed to be predominantly α-helical in its native state. On the other hand, monomeric Aβ is largely conformed as random coil in solution. The formation of Aβ dimmers coincides with the adoption of partial β structure. The Aβ dimmers assemble into higher order aggregates or oligomers, since there is a remarkable increase in the amounts of higher order aggregates and a decrease in the amount of dimmers. These higher order Aβ aggregates are protein micelles with a hydrophobic core and a polar exterior that appear as 3 nm spherical particles determined by atomic force or electron microscopy These higher order Aβ aggregates are protein micelles with a hydrophobic core and a polar exterior that appear as 3 nm spherical particles determined by atomic force or electron microscopy. At later times, these spherical shape particles appear to form curvilinear strings or "protofibrils". The protofibrils undergo a conformation change to form the straight, unbranched mature fibrils. Once the amyloid fibril lattice has been established, the fibril can grow by the addition of Aβ monomer or dimmer at the ends of the fibril. The higher order aggregates have molecular weights ranging from approximately 105 to 106 Da and with an average size corresponding to approximately 24 monomers. Aβ oligomers that appear as spherical particles are approximately 3 nm in diameter and have the characteristics of a protein amphipathic, since it lowers the surface tension of water. At longer incubation times, the oligomers also appear to co-aggregate to form curvilinear fibrils with a characteristic beaded appearance. The spherical oligomers and protofibrils appear to be intermediates in the pathway of fiber formation because they disappear as mature fibrils accumulate and the rate of monomer dissociation from them is too slow to account for fibril growth. The transition appears to involve a major conformational change, because fluorescence quenching analysis indicates that the carboxyl terminus is highly shielded from the aqueous solvent in the soluble oligomeric state, whereas it is exposed to the solvent in the fibrillar state. Once the amyloid fibril lattice has been established, it can grow by the addition of monomers onto the ends of the fibrils **[8].** Molecular simulations offer a direct means of accessing the conformational states of the Aβ peptides in aqueous media. MD studies have suggested that Aβ peptides, rather than being entirely disordered, are usually able to sample sequence-specific secondary structures. Using chemical shifts calculated from replica exchange molecular dynamics simulations, Wood and Rothlisberger investigated the differences observed between theoretical studies and experiments. They showed that the assigned random coil structures often derive from an averaging of β-sheet, α-helical and random coil structures **[9].** Insertion of a bulky group or proline as β-sheet breaker within the self-recognition-derived peptide sequenc, KLVFF, has been demonstrated as effective in inhibiting amyloid aggregation. Furthermore, peptidic inhibitors were also reported that via stabilization of the helical structure in residues 13−23 of Aβ prevented the formation of neurotoxic aggregates **[9, 10].**
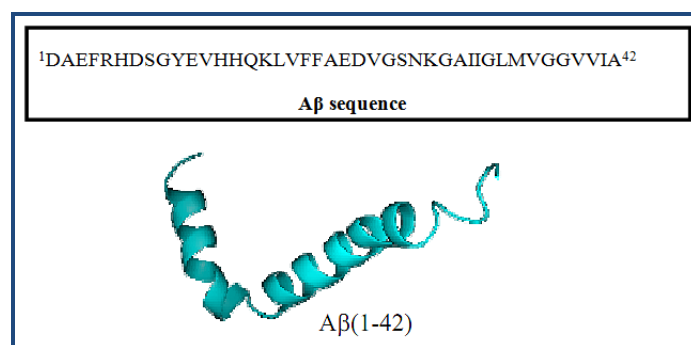

Figure 1: Amyloid Beta sequence and structure

Methodology:
Sequence & Structure
Solution NMR structure PDB 1IYT was taken from the RCSB Protein Data and employed as starting configurations for the MD simulations and other analysis **(Figure 1).**
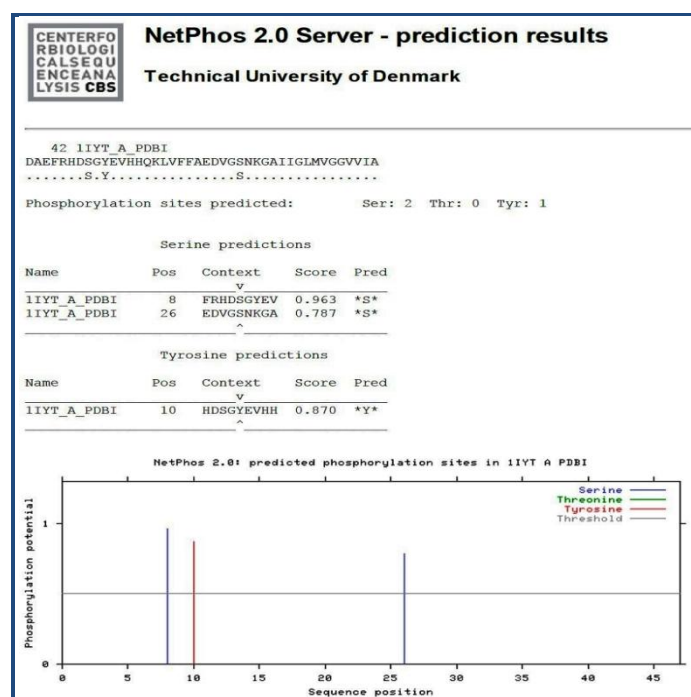

Figure 2: In silico analysis of putative phosphorylation sites of Aβ: Protein sequences of human Aβ1-42 sequences were analyzed by using NetPhos 2.0 computational prediction tool

(www.cbs.dtu.dk/services/NetPhos). The result from NetPhosK contains three parts for each of the protein/peptide sequence analyzed. The first part indicates the name, length of the aa sequence and predicted phospho sites (a). The second part shows the predicted phospho residues, their positions in the sequence and the respective phospho prediction score (b). The third part shows the graphical illustrations of phosphorylation potential of predicted phospho sites (c).
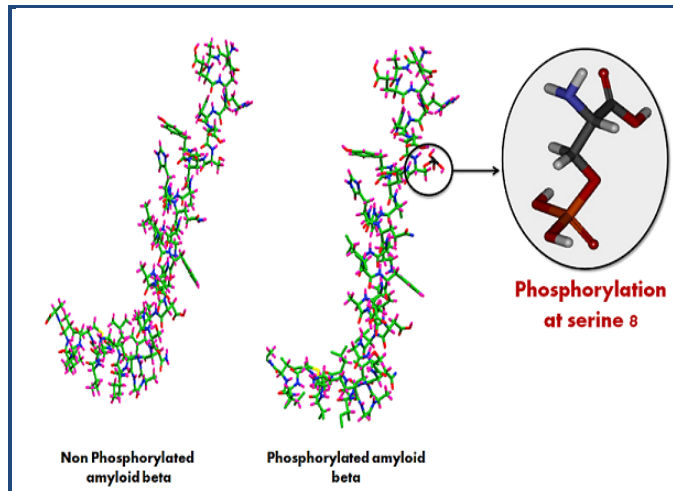
Figure 3: *In silico* phosphorylation of Aβ. Phosphate group was added on serine 8 using ArgusLab and making changes in the coordinate file. The above figure shows phosphorylated and non phosphorylated Aβ.
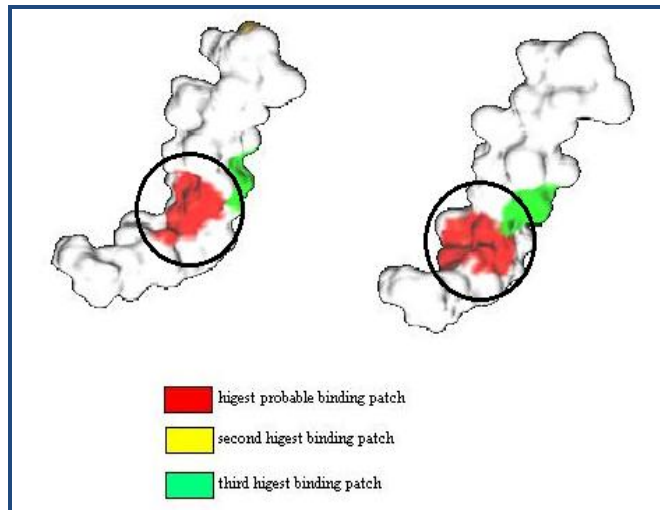

Figure 4: PPI-Pred Analysis- Shows that the binding patch is increased (red) in case of pAβ which depicts that pAβ will interact more efficiently.

NetPhos Server & Phosphorylation

The identification of the phosphorylation sites of Aβ was carried out using NetPhosK 1.0 (Blom et al., 1999), and NetPhos 2.0 sever (Blom et al.,2004) **(Figure 2).** These two prediction programmes employ neural network based algorithms prediction processes which are based on the evolutionary information obtained from sequence similarity of the phosphorylation site and taxonomy. The NetPhosK 1.0 is a kinase specific eukaryotic phosphorylation site predictions server. The kinase predictions are verified with homologues

phosphorylation sites obtained from other protein homologues from higher eukaryotes. The NetPhos 2.0 server is a generic (non kinase specific) phosphorylation predictions server and perform the predictions for serine, threonine and tyrosine phosphorylation sites in protein/peptides. The input sequences of any protein/peptide in the one-letter amino acid code in FASTA format can be used for carrying out the predictions. The instructions for the usage of the programme are provided with the respective tools. In-silico phosphorylation of Aβ was done using ArgusLab 4.0.1. and also by making changes in the coordinate file.
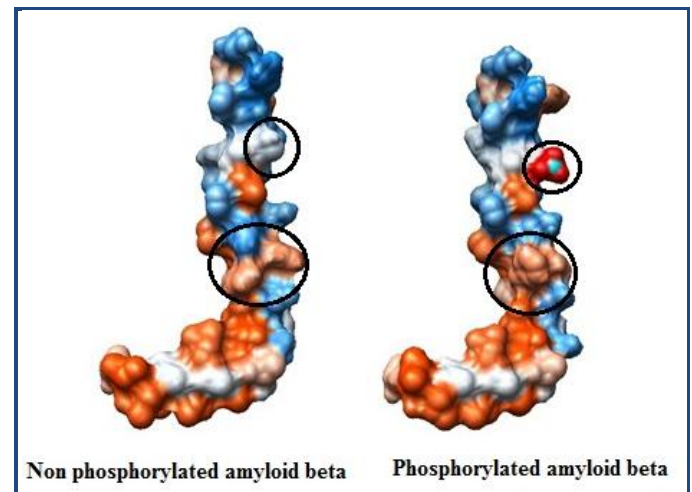
Figure 5: Hydrophobicity comparision: Phosphorylation of amyloid beta increases the hydrophobicity of the binding site (black circles) which means self aggregation of the peptide will be enhanced. RED and ORANGE regions are hydrophobic (UCSF Chimera Version. 1.6.2)
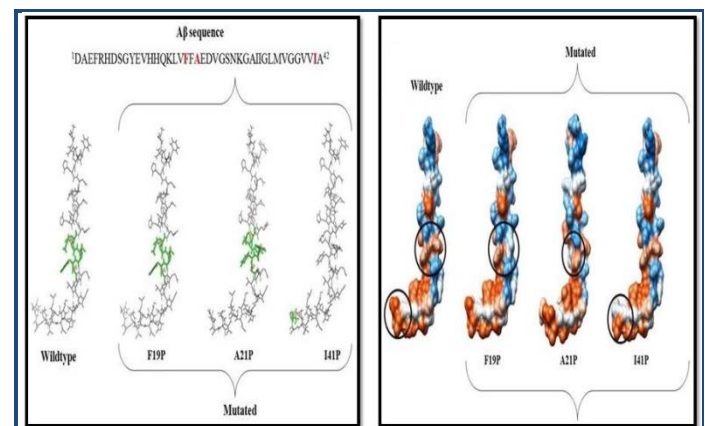
Figure 6: Residues 19, 21, and 41 are replaced by PROLINE to study the effect of mutants (Arguslab 4.0..1) and Comparing the hydrophobicity of the wildtype and mutants in UCSF Chimere Vers;ion. 1.6.2 reveleted that hydrophobicity of self-recognition site of the peptide was reduced with might reduce their aggregative ability.

Mutations & Hydrophobicity

The Aβ was mutated at residues 19, 21 and 41 using Swiss-PdbViewer 4.0.3. The energy of the mutant structure was minimised. The most probable binding sites for Aβ and its phosphorylated and mutant form was analysed using PPI-Pred (http://bmbpcu36.leeds.ac.uk/ppi_pred). The hydrophobicity

comparison between the three forms was carried out using chimera-1.6.2.

Simulation

Three molecular dynamic simulations, one for each form of Aβ was performed for 25 ns using GROMOS96. GROMOS ffG53a6 force field was used. The peptide was cantered in a cubic simulation box with a 1 nm distance allowed between the peptide and the edges of the box treated with periodic boundary conditions. The particle mesh Ewald method was employed for treating long-range electrostatics with a 1.4 nm cutoff for calculating short-range forces. After steepest descent energy minimization in vacuo, the box was solvated with the SPC explicit water model, and Na+ and Cl− ions were added to obtain a NaCl concentration of 150 mM and to achieve charge neutrality. The solvated peptide was then minimized using both steepest descent and conjugate gradient energy minimization methods. We performed a 100 ps equilibration dynamics (NVT/NPT) in which the water molecules were allowed to equilibrate around the restrained peptide atoms, in the process removing bad contacts and bringing the system near equilibrium conditions for the subsequent production MD run. For the equilibration step, the system was coupled to a Berendsen thermostat and barostat. The restraints were subsequently turned off, and a 25 ns production run was performed at 300 K in an NPT ensemble with temperature and pressure modulated by coupling to a Nosé−Hoover thermostat and a Parrinello−Rahman barostat, respectively. The neighbor list was generated every 10 ps, with a cutoff of 1.4 nm, and coordinates were saved every 20 ps. Pymol was used for the visualization of the simulation results.
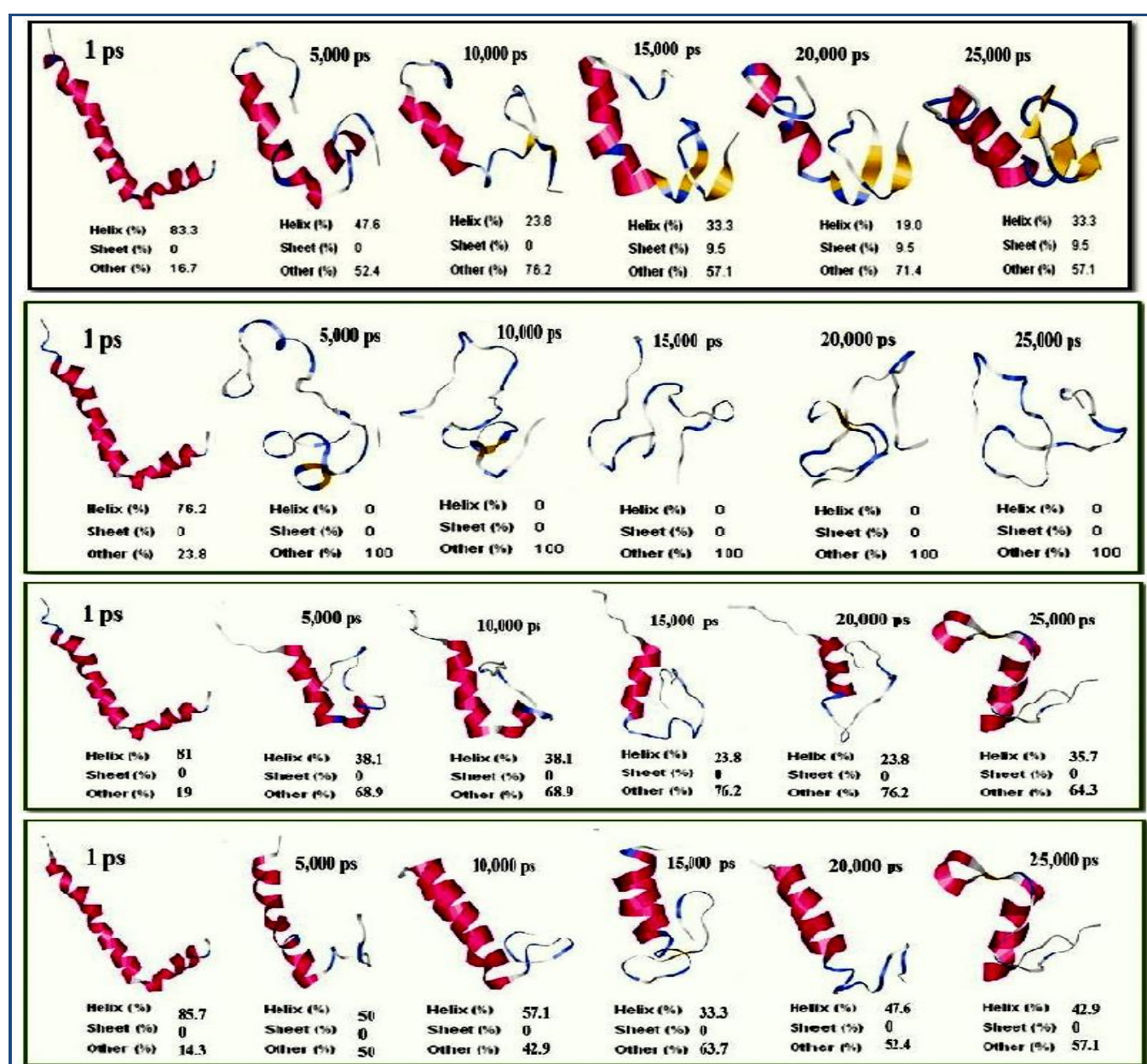
Figure 7: Shows secondary structure transition in wild type, mutant F19P, mutant F21P, MUTANT 141P respectively during 25ns MD Simulations using the GROMS forcefiedl ffG53a6. Thr helical peptide is converting into parallel beat sheet. The three state Composition was predicted using DSSP server. (http://2struc.cryst.bbk.ac.uk/twostruc).
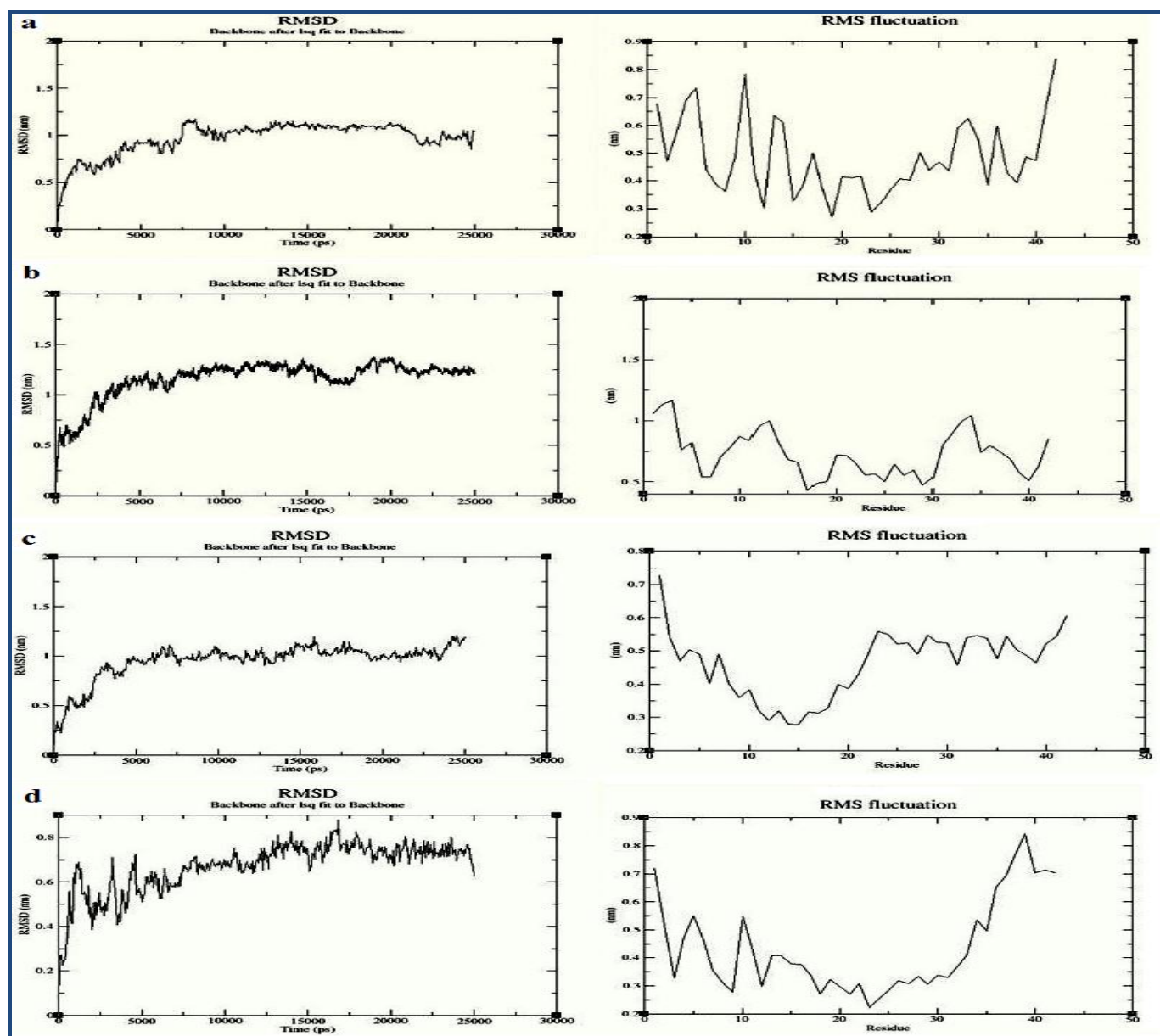
Figure 8: RMSD's of the wild type, mutant F19P, mutant F21P, mutant 141P respectively trajectories plotted vs time and RMSF plot for each residue of wild type, mutant F21P, mutant 141P respectively.

Secondary Structure

Dictionary of Secondary Structure of Proteins (DSSP) (http://2struc.cryst.bbk.ac.uk/about /) was used to analysise the secondary structure conformation of the wildtype and mutant Aβ after simulation.

Results:

Prediction of putative phosphorylation sites of Aβ

The preliminary identification of the putative phosphorylation sites of Aβ and identification of the responsible kinases were carried out by *in silico* analysis using freely available world wide web (www) based Netphos2.0 computational tool (www.cbs.dtu.dk/services/NetPhos). The results from the *in silico* analysis indicate that Ser-8, Ser-26 and Tyr-10 residues might be potential phosphorylation sites in Aβ sequence. The serine at 8th position had the highest prediction score of 0.963.

The serine at 26th position had a prediction score of 0.787. The tyrosine at 10th position has a score of 0.870 **(Figure 2)**

Phosphorylation of Aβ

The Aβ sequence contains two serine residues at 8th and 26th position, a tyrosine residue at 10th position which could possibly undergo phosphorylation. The primary goal of this work was to identify the role of phosphorylation in Aβ aggregation and pathogenesis of AD. Therefore, investigations were carried out to predict/identify/determine putative phosphorylation sites of Aβ. Phosphate group was added on serine 8 using ArgusLab **(Figure 3)**. PPI-pred analysis shows that the binding patch is increased (red) in case of pAβ which depicts that pAβ will interact more efficiently **(Figure 4)**. Phosphorylation of amyloid beta increases the hydrophobicity of the binding site (black circles) which means self aggregation

of the peptide will be enhanced. RED and ORANGE regions are hydrophobic **(Figure 5)**.

Discussion:

The current investigation was aimed at understanding the role of extracellular phosphorylation and mutation of Aβ peptide in aggregation. The aggregation of Aβ peptides is significantly related to the pathogenesis of neuronal degeneration in AD. Despite many previous studies on the structural analysis of Aβ aggregates, the precise mechanism has not yet been clarified. To obtain information on the structure of Aβ42 fibrils, we performed *in-silico* phosphorylation as well as proline replacement in Aβ peptide. The aggregative ability of the modified forms was analysed by hydrophobicity comparison and molecular dynamics. The analysis gave an insight into the role of phosphorylation at serine 8 which is capable of enhancing the propensity of Aβ to adopt a β-sheet rich conformation due increase in the hydrophobicity in binding sites. The phosphorylation induced β-sheet rich structures may accelerate the formation of small oligomeric aggregates that might seed aggregation into larger oligomeric and fibrillar assemblies. Phosphorylation of Ser8 negatively regulates Aβ degradation. It decreases the clearance by microglial cells and thus promotes its aggregation. Thus the inhibition of extracellular Aβ phosphorylation might play a role in the therapy and/or prevention of AD.

This analysis also sheds light on the effect of mutation in Aβ. Proline-substituted mutants of Aβ42 were formed *in-silico* and their aggregative ability was studies using MD simulation. The analysis revealed that F19P-, and F21P-Aβ42 did not form β-sheet therefore their aggregative ability was reduced. Whereas Aβ42 formed β-sheets thus they aggregated far more rapidly than the mutant forms.

Previous studies revealed that the C-terminal two residues of Aβ42 play a critical role in its aggregative ability and neurotoxicity. Weinreb *et al.* proposed the "hypothesis of hydrophobic cluster," stating that hydrophobic interaction among the side chains at the C terminus induces aggregation. In this hypothesis, Ile-41 is incorporated in the hydrophobic core formed by Leu-34 and Met-35. To confirm the role of the hydrophobic side chains at the C terminus of Aβ42, the hydrophilic threonine mutants at positions 41 or 42 (I41T- and A42T-A_42) were prepared and examined for their aggregative ability and neurotoxicity. Both I41T- and A42T-Aβ42 aggregated rapidly similar to wild-type Aβ42. Substitution with Thr did not abolish their cytotoxic effects **[11].**

Thus in this work C-terminal residue Ile 41 was also replaced by proline to find out whether C-terminal residues participates in the β-sheet formation. MD simulation was performed for the mutant to test the aggregative ability and neurotoxicity. The analysis revealed that the mutant did not form β-sheet therefore their aggregative ability was reduced. However, the C-terminal structure in the Aβ40 aggregation model is quite different from that of Aβ42. Our analysis data indicated that the C-terminal residues adopt a β-sheet structure thus helps in aggregation because of which Aβ40 aggregates far more slowly than Aβ42.

Conclusion:

Beta sheet is responsible for the formation of aggregates of Beta Amyloid (Aβ) in the Brain cells and since Proline (P) is a Beta sheet breaker, so Proline was used in order to reduce the Beta sheet formation and thus to reduce its aggregation too **(Figure 6)**. Simulation of Wild type Beta amyloid at 25 nano second by using Gromacs shows that Beta sheet is formed at the rate of 9.5% while for mutant Beta Amyloid i.e. F19P, F21P and I41P, Beta sheet formation was decreased to Zero **(Figure 7 & 8).** Thus mutation (substitution of Proline) at position 19, 21 and 41 show the null Beta sheet formation thus resulting to no aggregation of Beta Amyloid and thus can be employed for the treatment of Alzheimer disease.

References:

[1] Parvathy S & Buxbaum JD, Molecular Genetics of Alzheimer Disease, Neuropsychopharmacology: The Fifth Generation of Progress Davis KL, Charney D, Coyle JT, Nemeroff C, (Editors.) Lippincott, Williams, & Wilkins (Publisher) Philadelphia, Pennsylvania, 2002 [http://www.acnp.org/publications/neuro5thgeneration.aspx]

[2] Ehehalt R *et al. J Cell Biol.* 2003 **160**: 113 [PMID: 12515826]

[3] Wilquet V & De Strooper B, *Curr Opin Neurobiol*. 2004 **14:** 582 [PMID: 15464891]

[4] Iversen LL *et al. Biochem J.* 1995 **311:** 1 [PMID: 7575439]

[5] Teplow DB *et al. Acc Chem Res*. 2006 **39:** 635 [PMID: 16981680]

[6] Hoyer W *et al. Proc Natl Acad Sci U S A*. 2008 **105**: 5099 [PMID: 18375754]

[7] Urbanc B *et al. Biophys J.* 2004 **87**: 2310 [PMID: 15454432]

[8] http://scholarcommons.usf.edu/etd/2942/

[9] Olubiyi OO & Strodel B, *J Phys Chem B*. 2012 **116**: 3280 [PMID: 22300010]

[10] Karen E, *The Open Biology Journal* 2009 **2:** 185

[11] Morimoto A *et al. J Biol Chem.* 2004 **279**: 52781 [PMID: 15459202]